Identification of the thermal growth characteristics of coagulated tumor tissue in laser-induced thermotherapy[1]

Dietmar Hömberg[2], Jijun Liu[3], and Nataliya Togobytska[2]

[2] Weierstrass Institute, Mohrenstr. 39, 10117 Berlin, Germany
dietmar.hoemberg@wias-berlin.de, nataliya.togobytska@wias-berlin.de

[3] Southeast University, Department of Mathematics, Nanjing 210096, Republic of China
jjliu@seu.edu.cn

2010 Mathematics Subject Classification. 35R30, 74F05, 74N99.

Key words and phrases. Inverse problem, nonlinear equation, optimal control, iteration scheme, coupled system, numerics.

[1]The paper was finished during a stay of the first author at Southeast University, Nanjing. The second author is supported by NSFC(No.10771033), who also thanks WIAS, Berlin for its support during his short stays in 2009 and 2010. This work has been partially supported by the DFG Research Center Matheon "Mathematics for key technologies" in Berlin.

Abstract

We consider an inverse problem arising in laser-induced thermotherapy, a minimally invasive method for cancer treatment, in which cancer tissues is destroyed by coagulation. For the dosage planning numerical simulation play an important role. To this end a crucial problem is to identify the thermal growth kinetics of the coagulated zone. Mathematically, this problem is a nonlinear and nonlocal parabolic heat source inverse problem. The solution to this inverse problem is defined as the minimizer of a nonconvex cost functional. The existence of the minimizer is proven. We derive the Gateaux derivative of the cost functional, which is based on the adjoint system, and use it for a numerical approximation of the optimal coefficient.

1 Introduction

Laser-induced thermotherapy (LITT) is an advanced technique for cancer treatments, which is of minimally invasion and especially applicable for patients with liver metastases from colorectal primal tumors. In this technique, a catheter is used to place an applicator device connected to a laser source into the tumor (cf. Fig. 1). The energy of the laser light emitted from the surface of the applicator is absorbed by the biological tissue and therefore leads to a rise in temperature. The laser power and treatment time is adjusted such that a temperature of around 60^oC is reached in a neighborhood of the applicator. Driven by this rise in temperature the tissue is coagulated, a process which is governed by protein denaturation leading to the disruption of cell walls and eventually to the destruction of the tumor tissue. The deadened tissue remains in the body and is either decomposed or encapsulated.

The LITT treatment is guided using magnetic resonance imaging (MRI). Unfortunately, MRI is known to have either a good spatial or a good temporal resolution, making it difficult to predict the final size of the coagulated zone. Hence, there is a strong demand for computer simulations of LITT to support therapy planning and finding an optimal dosage.

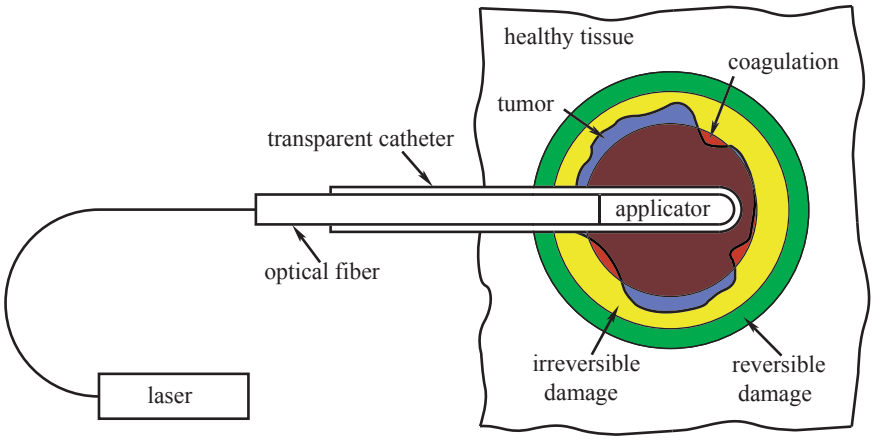

Figure 1: Sketch of laser-induced thermotheraphy treatment.

A detailed mathematical model for LITT is discussed in [6]. The most important parts are a coagulation model coupled to the bioheat equation describing temperature changes $\theta(x,t)$ in tumor tissue Ω. In laser medicine, coagulation is defined as an optically visible irreversible cell destruction (necrosis) caused by the denaturation of proteins. Following [11]

with an Arrhenius formalism model, the distribution of native tissue $z(x,t)$ for each protein is governed by the ordinary differential equation

$$\frac{\partial z_i(x,t)}{\partial t} = -F_i(\theta) z_i(x,t), \quad t > 0 \tag{1.1}$$

with the initial distribution

$$z_i(x,0) \equiv 1 \tag{1.2}$$

for all $x \in \Omega$, where the function $F_i(\cdot)$ describes the coagulation process, which has the representation for specified protein

$$F_i(\theta) = \begin{cases} 0, & \theta < 44C \\ A_i \exp\left(\frac{-G_i}{R\theta}\right), & \text{else,} \end{cases} \tag{1.3}$$

where two constants A_i, G_i depend on the properties of the protein and R is the universal gas constant. In this configuration, F_i can be considered either as a nonlinear functional with respect to θ or a function defined in $\Omega \times [0,T]$ in terms of the composition $F_i(\theta(x,t))$.

Although the above model with $F_i(\cdot)$ containing only two constants describing the coagulation process in each protein is quite simple, it is rather difficult to devise an experiment to identify the coagulation characteristics separately for each protein. Thus, it is more favourable to use a heuristic approach to model the tissue coagulation. To this end we weight several coagulation states of z_i for different proteins, with weights $c_i \in (0,1)$ representing the concentration of different proteins:

$$z(x,t) = \sum_{i=1}^{N} c_i z_i(x,t) \tag{1.4}$$

with $\sum_{i=1}^{N} c_i = 1$. Then the coagulation process for the biological tissue can be described as

$$\frac{\partial z(x,t)}{\partial t} = -G(\theta) z(x,t), \quad x \in \Omega, t > 0 \tag{1.5a}$$

$$z(x,0) = 1, \qquad x \in \Omega, \tag{1.5b}$$

where the non-negative function $G(\theta)$ describes the thermal part of the coagulation growth kinetics. Similar models are used in polymerization [1] and in solid-solid phase transitions [6]. The goal of this paper is to show how $G(\theta)$ can be identified from measurements.

The second physical quantity relevant for the treatment is the temperature $\theta(x,t)$ governed by the bio-heat equation. According to [11], for most of the biological tissue, the density ρ, the heat capacity c_p and the thermal conductivity k are almost constants in the relevant temperature interval between 37^oC and 70^oC. Then the bio-heat equation reads as follows

$$\frac{\partial \theta(x,t)}{\partial t} - \nabla \cdot \big(\kappa(x) \nabla \theta(x,t)\big) = Q(x,t,\theta), \quad x \in \Omega \times (0,T). \tag{1.6}$$

Here, T is the end-time of the treatment and $\kappa = k/\rho c_p$ is the thermal diffusivity. The heat source $Q = Q_L + Q_B$ in the bio-heat process contains two terms. The first term

Q_L describes the recalescence effect of the coagulation process, which is assumed to be proportional to the coagulation growth rate, i.e.

$$Q_L(x,t,\theta) = \beta \frac{\partial z}{\partial t}, \tag{1.7}$$

where $\beta > 0$ is the latent heat. Since $z_t \leq 0$, we observe that latent heat is consumed during the coagulation process. Neglecting metabolic changes, the second term Q_B describes the heat exchange due to blood perfusion in the tissue. A change in the blood perfusion rate is one of the reactions to the thermal changes in the tissue. Under the simple but widely used Pennes model to account for the blood perfusion with isotropic blood flow, this heat source can represented by

$$Q_B(x,t,\theta) = \tilde{\alpha}(z,x)(\theta_B - \theta), \quad \text{in } \Omega \times (0,T), \tag{1.8}$$

where θ_B is the known temperature of the arterial blood. Since there are no (active) vessels in the coagulated zone, there is no perfusion, hence we can write

$$\tilde{\alpha}(z,x) = z\alpha(x) \tag{1.9}$$

where $\alpha(x)$ describes the perfusion in the non-coagulated tissue.

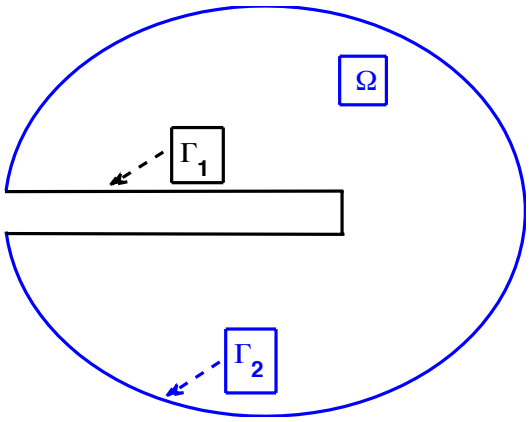

Figure 2: Physical domain and boundary parts.

The light is absorbed in a region around the catheter. The irradiation of laser light within the tissue can be described by the radiation transfer equation [3]. However, for our purposes it is sufficient to model it by a Neumann boundary condition, i.e., we have

$$-\kappa \frac{\partial \theta}{\partial \nu} = h(x,t), \quad \text{in } \Gamma_1 \times (0,T) \tag{1.10a}$$

$$-\kappa \frac{\partial \theta}{\partial \nu} = 0, \quad \text{in } \Gamma_2 \times (0,T) \tag{1.10b}$$

where Γ_1 is the boundary to the applicator and Γ_2 to the surrounding tissue, see Fig. 2. We also specify the initial temperature distribution

$$\theta(x,0) = \theta_0(x), \quad x \in \Omega. \tag{1.11}$$

We conclude that (1.5)-(1.11) constitute the laser-induced thermotherapy model. Note that similar models, in which a heat equation is coupled to a system of rate equations for

example arise in the modeling of phase transition in steel as well as in polymerization, see, e.g., [1, 6, 13].

As mentioned before, there is a strong demand for computer simulations of LITT supporting therapy planning and finding an optimal dosage. In order to perform numerical simulations which give quantitatively satisfactory results, the estimation of tissue parameters is a crucial task. However, while the respective data for the bio-heat equation are by now available, the determination of the parameters in the coagulation model is still an important task, in our case this is the function $G(\theta)$.

To this end, we specify the following measurement data

$$\theta(x,t) = F(x,t), \quad (x,t) \in \Gamma_1 \times (0,T). \tag{1.12}$$

From practical point of view this can be approximately realized by using temperature sensors in the catheter.

Then the purpose of this paper is to reconstruct $G(\theta)$ from some measurement information about the temperature, based on the over-determined system (1.5)-(1.12).

In the next section we will reformulate this problem in terms of an optimal control problem, the state system is analyzed in Section 3, while Section 4 is devoted to the control problem. Numerical results are given in Section 5. We would like to acknowledge that our analysis has been inspired by the investigations in [10, 9], where the identification of a temperature dependent heat coefficient has been studied.

2 Reformulation of the inverse problem

Thanks to the simplicity of the coagulation rate law (1.5) we easily obtain the solution

$$z(x,t) = \exp\left(-\int_0^t G(\theta(x,\tau))d\tau\right), \quad \text{in } \Omega \times (0,T). \tag{2.1}$$

On the other hand, a direct computation from (1.7)-(1.9) yields

$$Q(x,t,\theta) = z(x,t)\left(\alpha(x)(\theta_B - \theta) - \beta G(\theta)\right). \tag{2.2}$$

Therefore we get the following semilinear parabolic equation for $\theta(x,t)$ in $\Omega \subset \mathbb{R}^m$ ($m = 2,3$) with $\partial\Omega = \overline{\Gamma}_1 \cup \overline{\Gamma}_2$:

$$\frac{\partial\theta(x,t)}{\partial t} - \nabla\cdot\big(\kappa(x)\nabla\theta(x,t)\big) = e^{-\int_0^t G(\theta)d\tau}[\alpha(\theta_B - \theta) - \beta G(\theta)].$$

For given boundary and initial data $h(x,t)$ and $\theta_0(x)$, we are given the measurement data

$$\theta(x,t) = F(x,t), \quad x \in \Gamma_1,\ t \in (0,T). \tag{2.3}$$

The inverse problem is to identify $G(\theta)$, which belongs to the category of identifying the nonlinear heat source depending on the temperature.

We would like to mention that a laser material treatment problem with the source term $F(\theta(x,t)) + p(t)G(x,t)$ has been considered in [7], where the control term is $p(t)$, while the nonlinear function F is known. In our paper, the term $e^{-\int_0^t G(\theta)d\tau}$ in the right-hand side of the equation in (2.5) makes this problem nonlocal, which can be considered as a generalization of [7] in the sense that our source is nonlinear and nonlocal. Generally, it is very hard to

establish the uniqueness using finite measurement data. A known uniqueness result for the general nonlinear source for the heat system can be found in [8, Theorem 9.6.1], where the inversion input data are the Dirichlet-to-Neumann map in terms of the final measurements. In the case of recovering the coefficient $q(x)$ in the equation $u_t - \kappa\Delta u + q(x)u = 0$ with measurement data $u(x,T)$, the reconstruction based on the optimization can be found in [2].

For our problem (2.5)-(2.3), although the unknown nonlinear source G depends only on θ, the uniqueness is still open, noticing the nonlocal property of right-hand side of (2.5) and only one set of measurement data is specified. Therefore we introduce the cost functional

$$J(\theta, G) = \frac{1}{2}\int_0^T \int_{\Gamma_1} |\theta(x,t) - F(x,t)|^2 d\sigma dt \tag{2.4}$$

over some admissible set U_{ad} for G, where θ is the solution to direct problem for given G. Since it will be more convenient to deal with the original system instead of the nonlocal heat equation in terms of derivation of optimality conditions we will consider the following optimization problem and take its minimizer $\bar{G}$ as the solution to our inverse problem:

(CP) $\min J(\theta, G)$

subject to

$$\theta_t - \nabla\cdot\big(\kappa(x)\nabla\theta\big) = z[\alpha(\theta_B - \theta) - \beta G(\theta)], \quad \text{in } \Omega\times(0,T) \tag{2.5a}$$
$$z_t = -G(\theta)z, \quad \text{in } \Omega\times(0,T) \tag{2.5b}$$
$$-\kappa\frac{\partial\theta}{\partial\nu} = h, \quad \text{in } \Gamma_1\times(0,T) \tag{2.5c}$$
$$-\kappa\frac{\partial\theta}{\partial\nu} = 0, \quad \text{in } \Gamma_2\times(0,T) \tag{2.5d}$$
$$\theta(x,0) = \theta_0(x),\ z(x,0) = 1, \quad \text{in } \Omega, \tag{2.5e}$$

and the control constraint $G \subset \mathcal{G}_{ad}$.

For the admissible set we assume

$$\mathcal{G}_{ad} := \Big\{ G \in C^{1,\gamma}(\mathbb{R}) : \|G\|_{C^{1,\gamma}(\mathbb{R})} \le M_0, supp\ G \subset (\theta_-, \theta_+),\ G(s)|_{s\in\mathbb{R}} \ge 0 \Big\} \tag{2.6}$$

for some $\gamma \in (0,1)$, where θ_-, θ_+ are known constants. Furthermore we make the following assumptions for the data:

(A1) β, θ_B are positive constants

(A2) $\kappa \in L^\infty(\Omega)$ with $\kappa_1 \le \kappa(x) \le \kappa_2$ a.e. in Ω and constants $\kappa_2 \ge \kappa_1 > 0$

(A3) $\alpha \in L^\infty(\Omega)$, satisfying $\alpha \ge 0$ a.e. in Ω

(A4) $\theta_0 \in C(\bar{\Omega})$

(A5) $h \in L^\infty(0,T; L^p(\Gamma_1))$ with $p > m = \dim\Omega$

(A6) $F \in L^p(\Gamma_1\times(0,T))$.

3 Analysis of the state system

For the proof of our existence result we utilize the following maximal parabolic regularity result [5]:

Lemma 3.1. *Assume (A2), (A4), and (A5), let $p, s \in (1,\infty)$ and $f \in L^s(0,T;L^p(\Omega))$, then there holds:*

(1) *The parabolic system*

$$\theta_t - \nabla\cdot\big(\kappa(x)\nabla\theta\big) = f, \quad \text{in } \Omega\times(0,T) \tag{3.1a}$$

$$-\kappa\frac{\partial\theta}{\partial\nu} = h, \quad \text{in } \Gamma_1\times(0,T) \tag{3.1b}$$

$$-\kappa\frac{\partial\theta}{\partial\nu} = 0, \quad \text{in } \Gamma_2\times(0,T) \tag{3.1c}$$

$$\theta(x,0) = \theta_0 \quad , \text{ in } \Omega, \tag{3.1d}$$

has a unique solution in $W^{1,s}(0,T;L^p(\Omega))\cap L^s(0,T;W^{1,p}(\Omega))$ satisfying the apriori estimate

$$\|\theta\|_{W^{1,s}(0,T;L^p(\Omega))} + \|\theta\|_{L^s(0,T;W^{1,p}(\Omega))} \le C\big(\|f\|_{L^s(0,T;L^p(\Omega))} + \|h\|_{L^s(0,T;L^p(\Gamma_1))}\big).$$

(2) *If in addition $p > m$ and s has been chosen big enough, then there exists $\delta\in(0,1)$ such that $\theta\in C^{0,\delta}(\bar{Q})$ and it is bounded by the data as in the previous estimate.*

Remark 3.2. *This Lemma has been proven in [5]. For $p > m$ see Theorem 3.4 and 3.7 and for $p\in(1,m]$ see Remark 3.8.*

Since we have already seen that the rate law (1.5) admits an explicit solution (2.1), we can easily state the following

Lemma 3.3.

(1) *Let $\theta\in L^1(Q)$ and $G\in\mathcal{G}_{ad}$ then (1.5) admits a unique solution $z\in W^{1,\infty}(0,T;L^\infty(\Omega))$ such that*

$$0\le z(x,t)\le c_T < 1 \quad \text{a.e. in } Q.$$

Moreover, there exists $M>0$ independent of θ such that

$$\|z\|_{W^{1,\infty}(0,T;L^\infty(\Omega))}\le M.$$

(2) *Let $p\in(2,\infty)$ and $\theta_{1,2}\in L^p(Q)$ with solutions $z_{1,2}$ of (1.5). Then there exists a constant $L>0$ such that*

$$\|z_1 - z_2\|_{W^{1,p}(0,T;L^p(\Omega))}\le L\|\theta_1-\theta_2\|_{L^p(Q)}.$$

Part (2) can be easily proven testing the difference of (1.5) for $\theta_{1,2}$ by $|z_1-z_2|^{p-2}(z_1-z_2)$ and applying the inequalities of Gronwall and Young.

Defining $W_p^{1,1}(Q) = W^1(0,T;L^p(\Omega))\cap L^p(0,T;W^{1,p}(\Omega))$ we are now in a position to formulate the main result of this section:

Theorem 3.4. *Assume (A1)–(A4), then the state system (2.5) admits a unique solution (θ,z) such that $\theta\in W_p^{1,1}(Q)\cap C^{0,\delta}(\bar{Q})$ for some $\delta>0$ and $z\in W^{1,\infty}(0,T;L^\infty(\Omega))$.*

Proof. The proof is an easy application of the contraction mapping theorem. In view of Lemmas 3.3 and 3.1 the solution satisfies the apriori estimate

$$\|\theta\|_{W_p^{1,1}(Q)} \leq M, \tag{3.2}$$

where M only depends on h and θ_0. Hence we define the closed set

$$K = \{w \in W_p^{1,1}(Q) \,|\, \|w\|_{W_p^{1,1}(Q)} \leq M \text{ and } w(.,0) = \theta_0\}$$

and a mapping $F : \hat{\theta} \mapsto \theta$ where θ is the solution to (3.1) for

$$f = \hat{z}[\alpha(\theta_B - \hat{\theta}) - \beta G(\hat{\theta})]$$

where $\hat{z}$ is the solution to (1.5) for $\hat{\theta}$. Obviously, F maps K onto itself. Now let $\hat{\theta}_{1,2}$ be given and define $\theta = \theta_1 - \theta_2$ with $\theta_{1,2} = F(\hat{\theta}_{1,2})$. Then θ satisfies the system

$$\theta_t - \nabla \cdot \big(\kappa(x)\nabla\theta\big) = \bar{f}, \quad \text{in } \Omega \times (0,T) \tag{3.3a}$$

$$-\kappa \frac{\partial \theta}{\partial \nu} = 0, \quad \text{in } \partial\Omega \times (0,T) \tag{3.3b}$$

$$\theta(x,0) = 0, \qquad \text{in } \Omega, \tag{3.3c}$$

with $\bar{f} = \hat{z}_1[\alpha(\theta_B - \hat{\theta}_1) - \beta G(\hat{\theta}_1)] - \hat{z}_2[\alpha(\theta_B - \hat{\theta}_2) - \beta G(\hat{\theta}_2)]$. We apply Hölder's inequality and Lemma 3.3(2) to obtain

$$\|\bar{f}\|_{L^p(Q)} \leq c\|\hat{\theta}_1 - \hat{\theta}_2\|_{L^p(Q)} \leq cT^{\frac{p-1}{p}}\|\hat{\theta}_{1,t} - \hat{\theta}_{2,t}\|_{L^p(Q)} \leq cT^{\frac{p-1}{p}}\|\hat{\theta}_1 - \hat{\theta}_2\|_{W_p^{1,1}(Q)}. \tag{3.4}$$

Hence, F is a contraction for some $T^+ \leq T$ small enough and thanks to the global apriori estimate we can extend the solution to the whole time interval $[0,T]$. □

Thanks to this theorem we have a well-defined solution operator

$$S : \mathcal{G}_{ad} \ni G \mapsto \theta = \theta(G). \tag{3.5}$$

Next, we prove

Corollary 3.5. *Let*

$$\theta_+ > \max_{G \in \mathcal{G}_{ad}} \|\theta(G)\|_{C(\bar{Q})} \quad \text{and} \quad \theta_- < \theta_B \tag{3.6}$$

then

$$\theta_- < \theta(G)(x,t) < \theta_+ \quad \text{for all } (x,t) \in \bar{Q} \text{ and all } G \in \mathcal{G}_{ad}. \tag{3.7}$$

Proof. The upper bound is a direct consequence of Theorem 3.4, since the constant M in (3.2) is independent of G. To derive the lower bound we write

$$\theta = \theta_- + [\theta - \theta_-]_+ - [\theta - \theta_-]_-$$

where $[x]_+ = \max\{x, 0\}$ and $[x] = -\min\{x, 0\}$ are the positive and negative part functions, respectively. Then, by a standard argument we test (3.1) with $[\theta - \theta_-]_-$ to obtain

$$\begin{aligned}
&\frac{1}{2}\int_\Omega [\theta-\theta_-]_-^2 dx + \int_0^t\int_\Omega \kappa|\nabla[\theta-\theta_-]_-|^2 dxds = -\int_0^t\int_\Omega z\beta G(\theta)[\theta-\theta_-]_- dxds \\
&\quad + \int_0^t\int_\Omega z\alpha(\theta_B-\theta_-)[\theta-\theta_-]_- dxds + \int_0^t\int_\Omega z\alpha[\theta-\theta_-]_-^2 dxds \\
&\quad \le c\int_0^t\int_\Omega [\theta-\theta_-]_-^2 dxdt.
\end{aligned}$$

Invoking Gronwall's Lemma finishes the proof.

□

To investigate stability of solutions we take $G_{1,2} \in \mathcal{G}_{ad}$. Then the difference of corresponding solutions $\theta_{1,2}$ solves a system similar to (3.3) but with $\bar{f}$ given by

$$\bar{f} = z_1[\alpha(\theta_B - \theta_1) - \beta G_1(\theta_1)] - z_2[\alpha(\theta_B - \theta_2) - \beta G_2(\theta_2)].$$

Proceeding as in the proof of Theorem 3.4 we can estimate

$$\|\bar{f}\|_{L^p(Q)}^p \le c_1 T^{p-1}\int_0^t\int_0^s\int_\Omega (\theta_{1,\xi} - \theta_{2,\xi})^p dxd\xi ds + c_2\|G_1 - G_2\|_{C[\theta_-,\theta_+]}^p.$$

Utilizing Gronwall's Lemma once again together with Lemma 3.1 and 3.3(2), we obtain

Corollary 3.6. *Let $\theta_{1,2}$ and $z_{1,2}$ be the solutions to (2.5) corresponding to $G_{1,2} \in \mathcal{G}_{ad}$, then there exists a constant $L > 0$ such that*

$$\|\theta_1 - \theta_2\|_{W_p^{1,1}(Q)} + \|\theta_1 - \theta_2\|_{C^{0,\delta}(\bar{Q})} + \|z_1 - z_2\|_{W^{1,p}(0,T;L^p(\Omega))} \le c\|G_1 - G_2\|_{C[\theta_-,\theta_+]}.$$

Now, we show that the solution operator is also Gateaux-differentiable. To this end we take admissible functions G and $\bar{G}$, define

$$G^\varepsilon(\cdot) = \bar{G}(\cdot) + \varepsilon(G(\cdot) - \bar{G}(\cdot)), \tag{3.8}$$

and denote $(\theta^\varepsilon, z^\varepsilon)$, $(\bar{\theta}, \bar{z})$ the corresponding solutions. Formally, we define the derivatives as

$$\dot{\theta} = \lim_{\varepsilon\to 0}\frac{\theta^\varepsilon - \bar{\theta}}{\varepsilon}, \quad \dot{z} = \lim_{\varepsilon\to 0}\frac{z^\varepsilon - \bar{z}}{\varepsilon}. \tag{3.9}$$

From the definition of G^ε we have

$$\lim_{\varepsilon\to 0}\frac{G^\varepsilon(z^\varepsilon) - \bar{G}(\bar{\theta})}{\varepsilon} = \bar{G}'(\bar{\theta})\dot{\theta} + G(\bar{\theta}) - \bar{G}(\bar{\theta}).$$

Thus, formal computations lead to the system

$$\dot{\theta}_t - \nabla\cdot\left(\kappa(x)\nabla\dot{\theta}\right) = \dot{z}[\alpha(\theta_B - \bar{\theta}) - \beta\bar{G}(\bar{\theta})] \tag{3.10a}$$

$$+\bar{z}(-\alpha\dot{\theta} - \beta(\bar{G}'(\bar{\theta})\dot{\theta} + G(\bar{\theta}) - \bar{G}(\bar{\theta}))), \quad \text{in } \Omega\times(0,T) \tag{3.10b}$$

$$\dot{z}_t = -\bar{G}(\bar{\theta})\dot{z} - (\bar{G}'(\bar{\theta})\dot{\theta} + G(\bar{\theta}) - \bar{G}(\bar{\theta}))\bar{z}(x,t), \quad \text{in } \Omega\times(0,T) \tag{3.10c}$$

$$-\kappa\frac{\partial\dot{\theta}}{\partial\nu} = 0, \quad \text{in } \partial\Omega\times(0,T) \tag{3.10d}$$

$$\dot{\theta}(x,0) = 0,\ \dot{z}(x,0) = 0, \quad \text{in } \Omega, \tag{3.10e}$$

In the spirit of Theorem 3.4 one can easily verify that (3.10) admits a unique solution $(\dot\theta, \dot z) \in W_p^{1,1}(Q) \cap C^{0,\delta}(\bar Q) \times W^{1,\infty}(0,T;L^\infty(\Omega))$. To prove that this indeed is the Gateaux derivative, we define

$$\eta^\varepsilon = \theta^\varepsilon - \bar\theta - \varepsilon\dot\theta \quad \text{and} \quad \zeta^\varepsilon = z^\varepsilon - \bar z - \varepsilon \dot z.$$

Straightforward computations using a first-order expansion of G and $\bar G$ show that $(\eta^\varepsilon, \zeta^\varepsilon)$ solve the system

$$\eta_{\varepsilon,t} - \nabla\big(\cdot\,(k(x)\nabla\eta_\varepsilon\big) = g_1\eta_\varepsilon + g_2\zeta_\varepsilon + g_3(\varepsilon,x,t), \quad \text{in } \Omega\times(0,T) \tag{3.11a}$$

$$\zeta_{\varepsilon,t} = g_4\zeta_\varepsilon + g_5\eta_\varepsilon + g_6(\varepsilon,x,t), \quad \text{in } \Omega\times(0,T) \tag{3.11b}$$

$$-\kappa\frac{\partial\eta_\varepsilon}{\partial\nu} = 0, \quad \text{in } \partial\Omega\times(0,T) \tag{3.11c}$$

$$\eta_\varepsilon(x,0) = 0,\ \zeta_\varepsilon(x,0) = 0, \quad \text{in } \Omega. \tag{3.11d}$$

Here, g_i, $i = 1,\dots,6$ are bounded in $L^\infty(Q)$. Moreover, thanks to the stability result in Corollary 3.6, we have

$$\|g_3(\varepsilon,x,t)\|_{L^\infty(Q)} + \|g_6(\varepsilon,x,t)\|_{L^\infty(Q)} \le c\varepsilon^2,$$

with a constant $c > 0$. Now, we test (3.11b) with $|\zeta_\varepsilon|^{p-2}\zeta_\varepsilon$ and apply Youngs inequality, leading to

$$\int_\Omega |\zeta_\varepsilon|^p dx \le c_1 \int_0^t\int_\Omega |\zeta_\varepsilon|^p dxds + \frac{1}{p}\int_0^t\int_\Omega (g_5\eta_e + g_6)^p dxds + \frac{p-1}{p}\int_0^t\int_\Omega |\zeta_\varepsilon|^p dxds.$$

Gronwall's lemma and comparison in (3.11b) give

$$\|\zeta_\varepsilon\|_{W^{1,p}(0,T;L^p(\Omega))} \le c_2\|\eta_\varepsilon\|_{L^p(Q)} + c_3\varepsilon^2.$$

As in the proof of Theorem 3.4 we can now apply Lemma 3.1 and Gronwall to obtain

$$\|\eta_\varepsilon\|_{W_p^{1,1}(Q)} + \|\eta_\varepsilon\|_{C^{0,\delta}(\bar Q)} + \|\zeta_\varepsilon\|_{W^{1,p}(0,T;L^p(\Omega))} \le c\varepsilon^2. \tag{3.12}$$

Thus, we have proved

Theorem 3.7. *The solution operator $S : \mathcal{G}_{ad} \to W_p^{1,1}(Q) \cap C^{0,\delta}(\bar Q) \times W^{1,p}(0,T;L^p(\Omega))$ to (3.1) is Gateaux differentiable. The directional derivative $(\dot\theta, \dot z)$ in direction $G - \bar G$ is defined as the solution to (3.10).*

4 Analysis of the optimal control problem

To prove the existence of a solution to **(CP)** we proceed similar to [10] by introducing the set

$$\mathcal{T}_{ad} := \{(G, \theta(G)) : G \in U_{ad}, \theta \in C^{0,\delta}(\bar Q)\}.$$

Lemma 4.1. *$\mathcal{T}_{ad}$ is compact in $C^1[\theta_-,\theta_+] \times C(\bar Q)$.*

Proof. Standard embedding results for Hölder continuous functions imply that $\mathcal{T}_{ad}$ is a relatively compact subset of $C^1[\theta_-,\theta_+]\times C(\bar{Q})$. To show that it is also closed we take a a sequence $(G_n,\theta_n)\in\mathcal{T}_{ad}$ with limit (G,θ). Thanks to the uniqueness of solutions to the state system (2.5) passing to the limit in the equations in a standard way (see, e.g. [4]) yields $\theta=\theta(G)\in C^{0,\delta}(\bar{Q})$. Since also $G\in\mathcal{G}_{ad}$, this concludes the proof. □

Using Lemma 4.1 and the continuity of the cost functional$J(\theta(G),G)$ in U_{ad} together with Weierstrass' Theorem we obtain

Theorem 4.2. *The control problem* **(CP)** *has a solution* $\bar{G}\in\mathcal{G}_{ad}$.

In order to characterize the gradient of the cost functional it is convenient to introduce an adjoint system. To this end we employ a standard Lagrange technique (see, e.g. [12]), which results in the system

$$-\phi_t-\nabla\cdot\big(\kappa(x)\nabla\phi\big)=-\bar{z}(\alpha+\beta\bar{G}'(\bar{\theta}))\phi-\bar{G}'(\bar{\theta})\bar{z}\psi,\quad\text{in }\Omega\times(0,T)\tag{4.1a}$$

$$-\psi_t=-\bar{G}(\bar{\theta})\psi+[\alpha(\theta_B-\bar{\theta})-\beta\bar{G}(\bar{\theta})]\phi,,\quad\text{in }\Omega\times(0,T)\tag{4.1b}$$

$$-\kappa\frac{\partial\phi}{\partial\nu}=-(\bar{\theta}-F),\quad\text{in }\Gamma_1\times(0,T)\tag{4.1c}$$

$$-\kappa\frac{\partial\phi}{\partial\nu}=0,\quad\text{in }\Gamma_2\times(0,T)\tag{4.1d}$$

$$\phi(x,T)=0,\ \psi(x,T)=0,\qquad\text{in }\Omega,\tag{4.1e}$$

In view of (A6) we can again utilize Lemma 3.1 and argue similar to the proof of Theorem 3.4 to show that 4.1 admits a unique solution $(\phi,\psi)\in W_p^{1,1}(Q)\cap C^{0,\delta}(\bar{Q})\times W^{1,\infty}(0,T;L^\infty(\Omega))$.

Now let $\bar{G}$ be a local minimizer of $J(\theta(\cdot),\cdot)$, then we have

$$\begin{aligned}0\ &\le\ \lim_{\varepsilon\to0}\frac{J(\theta(G^\varepsilon),G^\varepsilon)-J(\theta(\bar{G}),\bar{G})}{\varepsilon}\\ &=\ \frac{1}{2}\lim_{\varepsilon\to0}\frac{\int_0^T\int_{\Gamma_1}[(\theta^\varepsilon-F)^2-(\bar{\theta}-F)^2]}{\varepsilon}=\int_0^T\int_{\Gamma_1}(\bar{\theta}-F)\dot{\theta}d\sigma dt=:I.\end{aligned}\tag{4.2}$$

Next, we test (4.1a) with $\dot\theta$ and integrate by parts with respect to time yielding

$$
\begin{aligned}
I \quad &= \int_0^T\int_\Omega \dot\theta_t\phi\,dxdt + \int_0^T\int_\Omega \big(\bar z(\alpha+\beta\bar G'(\bar\theta))\dot\theta\phi + \bar G'(\bar\theta)\bar z\psi\big)\dot\theta\,dxdt \\
&\quad + \int_0^T\int_\Omega \kappa\nabla\phi\cdot\nabla\dot\theta\,dxdt \\
&\overset{(3.10a)}{=} \int_0^T\int_\Omega \phi\dot z[\alpha(\theta_B-\bar\theta)-\beta\bar G(\bar\theta)]\,dxdt - \int_0^T\int_\Omega \phi\bar z\beta[G(\bar\theta)-\bar G(\bar\theta)]\,dxdt \\
&\quad + \int_0^T\int_\Omega \bar z\bar G'(\bar\theta)\psi\dot\theta\,dxdt \\
&\overset{(3.10c)}{=} \int_0^T\int_\Omega \phi\dot z[\alpha(\theta_B-\bar\theta)-\beta\bar G(\bar\theta)]\,dxdt - \int_0^T\int_\Omega (\beta\phi+\psi)[G(\bar\theta)-\bar G(\bar\theta)]\bar z\,dxdt \\
&\quad + \int_0^T\int_\Omega \dot z\psi_t\,dxdt - \int_0^T\int_\Omega \bar G(\bar\theta)\dot z\psi\,dxdt \\
&\overset{(4.1b)}{=} -\int_0^T\int_\Omega (\beta\phi+\psi)[G(\bar\theta)-\bar G(\bar\theta)]\bar z\,dxdt.
\end{aligned}
$$

All in all we have derived the following necessary optimality conditions:

Theorem 4.3. *There exists an optimal control $\bar G\in\mathcal{G}_{ad}$, an optimal state $(\bar\theta,\bar z)$ satisfying the state system (2.5) and an adjoint state (ϕ,ψ) satisfying (4.1). In addition, the following variational inequality holds:*

$$
-\int_0^T\int_\Omega (\beta\phi+\psi)[G(\bar\theta)-\bar G(\bar\theta)]\bar z\,dxdt \ge 0 \qquad \text{for all } G\in\mathcal{G}_{ad}. \tag{4.3}
$$

5 Numerical simulation

5.1 The state equation

Numerical tests showed that the simulation results obtained in [3] for the full system including the radiation transport can be approximated in a more realistic way by choosing a distributed heat source with support in the neighborhood of the applicator. Hence the following system is the basis for the simulations:

$$
\begin{aligned}
\theta_t - \nabla\cdot\big(\kappa(x)\nabla\theta\big) &= z[\alpha(\theta_B-\theta)-\beta G(\theta)]+\gamma\Phi, && \text{in } \Omega\times(0,T) && \text{(5.1a)}\\
z_t &= -G(\theta)z, && \text{in } \Omega\times(0,T) && \text{(5.1b)}\\
-\kappa\frac{\partial\theta}{\partial\nu} &= 0, && \text{in } \partial\Omega\times(0,T) && \text{(5.1c)}\\
\theta(x,0)=\theta_0(x),\ z(x,0) &= 1, && \text{in } \Omega, && \text{(5.1d)}
\end{aligned}
$$

The heat source in (5.1) is approximated as

$$\Phi(x,y) = \begin{cases} e^{-6000(x^2+y^2)}, & x \geq 0 \\ e^{-6000y^2}, & \text{else.} \end{cases}$$

The physical constants used for the simulations are summarized in Table 1. Note that the whole setting has been taken from an experiment reported in [11].

Symbol	Units	native and coagulated tissue
ρ	$kg \cdot m^{-3}$	1040
c_p	$Jkg^{-1}K^{-1}$	3640
κ	$Wm^{-1}K^{-1}$	0.518
θ_B	K	310.15
α	$Jm^{-3}K^{-1}s^{-1}$	$6.7 \cdot 10^5$
β	Jm^{-3}	10^{-4}
γ	m^{-1}	19.5

Table 1: Data used in the simulations (from [11]).

We have approximated the forward problem with a function $G(\theta) = 0.01e^{-0.02(\theta-338.15)^2}$ and initial temperature $\theta_0 = 37$ °C with linear finite elements using the MATLAB pde toolbox. Figure 3 depicts the function $G(\theta)$. The corresponding temperature distribution and the coagulated tissue at $t = 600s$ i.e. at the end of the exposure time are shown in Figure 4. The maximal temperature is 89.9 °C.

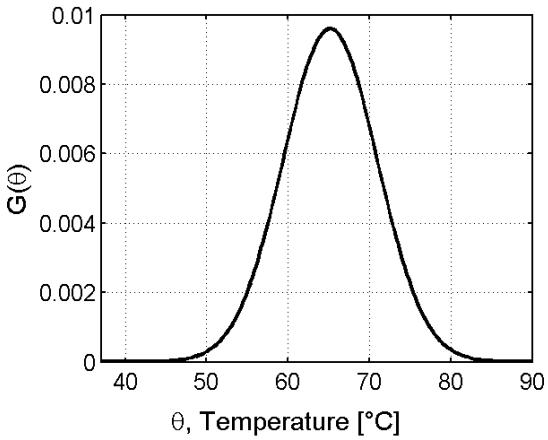

Figure 3: Function $G(\theta)$.

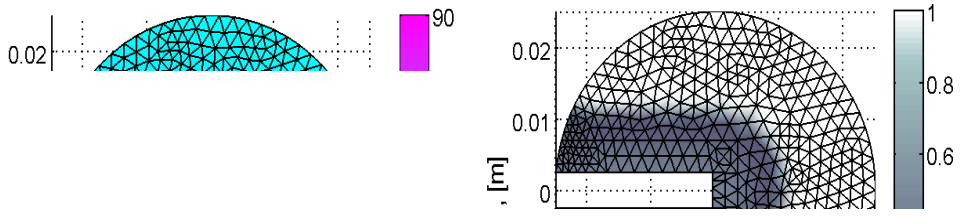

Figure 4: Simulated temperature distribution (left) and coagulated tissue (right) at the end time $t = 600s$.

A convenient way to reduce the computational effort for the identification problem is to nondimensionalize the problem first. To this end we introduce the following transformations:

$$\begin{aligned}
\hat{x} &= \frac{x + 0.025}{0.05}, \\
\hat{y} &= \frac{y + 0.025}{0.05}, \\
\hat{\theta} &= \frac{\theta - 310.15}{53}, \\
\hat{z} &= z, \\
\hat{t} &= \frac{t}{600}.
\end{aligned}$$

Then the transformed state system is given by

$$\hat{\theta}_{\hat{t}} - \hat{\kappa}\Delta\hat{\theta} = -\hat{\alpha}\hat{z}\theta + \hat{\beta}\frac{\partial\hat{z}}{\partial\hat{t}} + \hat{\gamma}\Phi(\hat{x},\hat{y}), \qquad \text{in } \hat{\Omega}\times(0,\hat{T}) \tag{5.2a}$$

$$\frac{\partial\hat{z}}{\partial\hat{t}} = -\hat{G}(\hat{\theta})\hat{z}, \qquad \text{in } \hat{\Omega}\times(0,\hat{T}) \tag{5.2b}$$

$$-\hat{\kappa}\frac{\partial\hat{\theta}}{\partial n}(\hat{x},\hat{t}) = 0, \qquad \text{in } \partial\hat{\Omega}\times(0,\hat{T}), \tag{5.2c}$$

$$\hat{\theta}(\hat{x},0) = 0, \qquad \text{in } \partial\hat{\Omega}, \tag{5.2d}$$

$$\hat{z}(\hat{x},0) = 1, \qquad \text{in } \partial\hat{\Omega}, \tag{5.2e}$$

where the transformed constants are summarized in Table 2. To generate model data for the identification problem, we have solved the system of state equations (5.2a)-(5.2e) with a function $\hat{G}(\theta)$ depicted in Figure 5, initial temperature $\hat{\theta}_0 = 0$ and treatment time $\hat{T} = 1$. Figure 6 shows the corresponding temperature distribution and the coagulated tissue at $\hat{T} = 1$ i.e. at the end of the exposure time.

Compared to the previous simulation prior to nondimensionalization the coagulated fraction is smaller, however in terms of solving the identification problem this is not important.

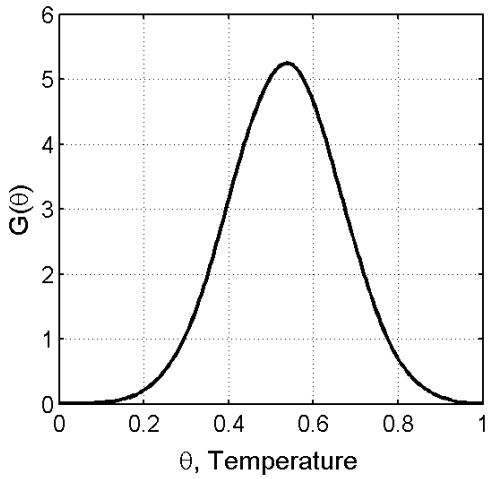

Figure 5: Function $G(\theta)$.

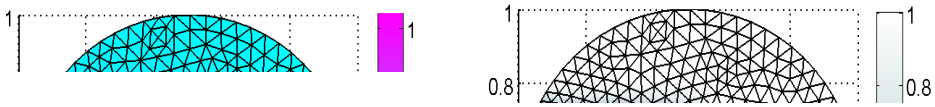

Figure 6: Simulated temperature distribution (left) and coagulated tissue (right) at the end time $\hat{t}_e = 1$.

Symbol	Native and coagulated tissue
$\hat{\kappa}$	0.0328
$\hat{\alpha}$	106.21
$\hat{\beta}$	$4.98 \cdot 10^{-13}$
$\hat{\gamma}$	40.82

Table 2: Value of constants in transformed state system.

5.2 Numerical solution of the identification problem

Due to the structure of the problem we cannot give a characterization of the gradient in function space. Hence we proceed as follows. First , we discretize the control G. We partition the domain $[\theta_-, \theta_+]$ by

$$\theta_- := \tau_0 < \tau_1 < \cdots < \tau_N := \theta_+$$

and use cubic B-splines with basis functions $\varphi_i(\tau)$ with $i = 1, \cdots, N$ to approximate G, i.e.,

$$G^N(\tau) = \sum_{i=1}^{N} G_i \varphi_i(\tau), \quad \tau \in [\theta_-, \theta_+].$$

Introducing the finite-dimensional set of admissible controls,

$$G_{ad}^N = \{G^N = (G_1, \ldots, G_N)^T \in \mathbf{R}^{N+1} \,|\, 0 \le m_1 \le G_i \le M_1 \text{ for } i = 1, \cdots, N\}$$

we can replace **(CP)** by the corresponding finite-dimensional optimization problem $\mathbf{(CP)}_N$. To compute the gradient of the reduced cost functional $j(\bar{G}^N) = J(\theta(\bar{G}^N), \bar{G}^N)$ we choose G^N in (4.3) such that $G_j = \bar{G}_j$ for $j \neq l$. Then the inequality boils down to

$$-(G_l - \bar{G}_l) \int_0^T \int_\Omega (\beta\phi + \psi)\bar{z}\varphi_l(\bar{\theta})\, dxdt \ge 0.$$

For $\bar{G}_i \neq m_1, M_1$, we thus obtain the gradient of $j(G^N)$ as

$$\frac{\partial j}{\partial G_l} = -\int_0^T \int_\Omega (\beta\phi + \psi)\bar{z}\varphi_l(\bar{\theta})\, dxdt, \quad 1 \le l \le N. \tag{5.3}$$

Using this gradient we have solved the resulting nonlinear optimization problem with a BFGS method using the MATLAB routine *fmincon*. The upper and lower bounds in the control constraints have been chosen as $M_1 = 10, m_1 = 0$, respectively. Figure 7 shows four iterations in the case of unperturbed data. The resulting convergence history is given in Table 3.

To investigate the stability of our method with respect to noisy data we have perturbed the model data with 10% and 30 % noise, respectively. Note that these values correspond to 1% noise and 5% noise, respectively, for the original problem, i.e. prior to nondimensionalization. From the results, depicted in Figure 8, we conclude that our approach is stable with respect to perturbed data.

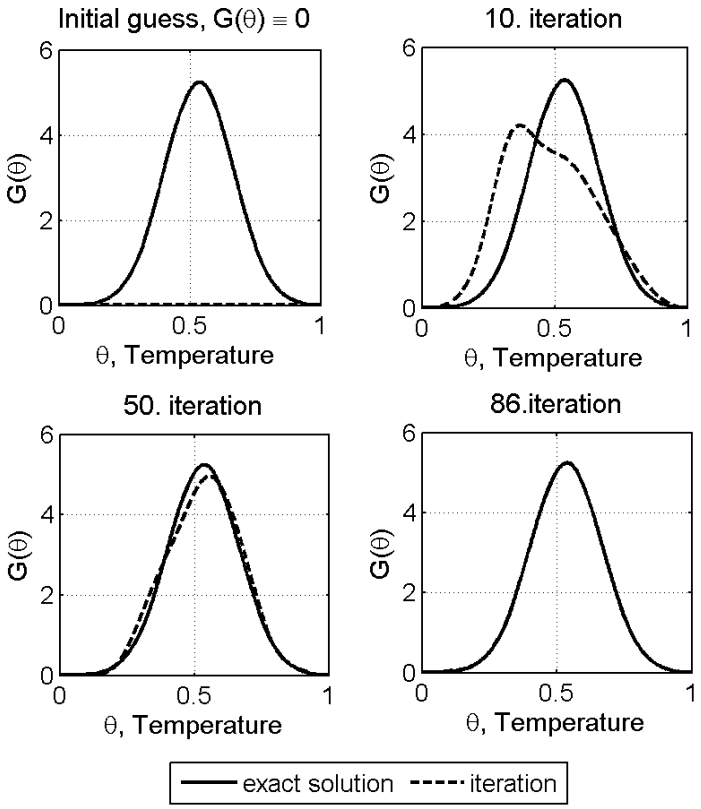

Figure 7: Iterations of optimisation procedure.

Iteration	J_i	e_i
1	6.6483	66.2174
20	0.0068	18.7427
40	0.0025	13.1533
60	$1.9593 \cdot 10^{-6}$	0.0288
86	$3.0419 \cdot 10^{-9}$	0.0014

Table 3: Value of objective function J_i and error in the parameter $e_i = \|G^*(\theta) - G_i(\theta)\|$ of i-iteration.

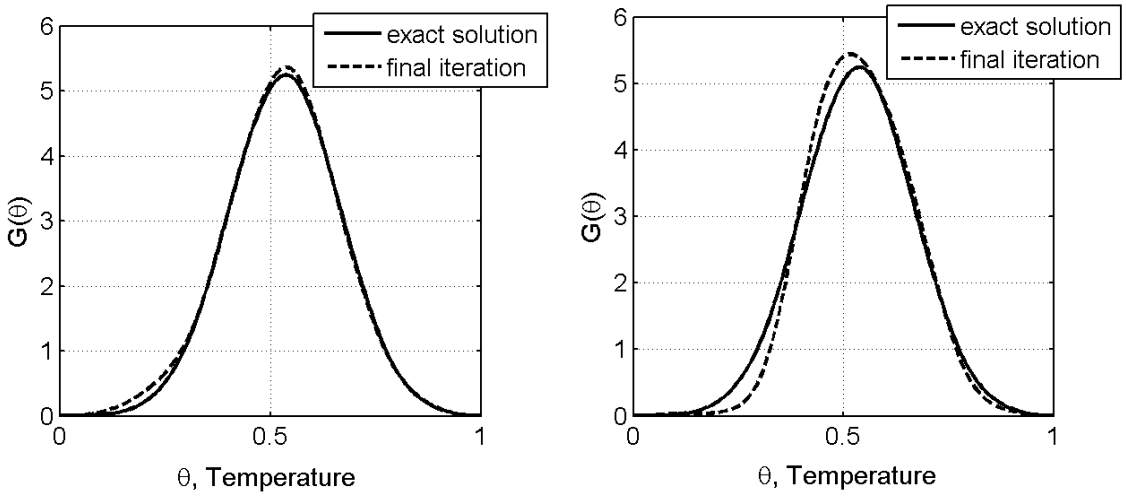

Figure 8: Final iteration of optimisation procedure. Identification of $G(\theta)$ from the data with 10 % noise (left) and 30 % noise (right).

References

[1] Andreucci, D., Fasano, A., Primicerio, M., *On a Mathematical Model for the Crystallization of Polymers*, in: O'Malley, R.E. (Ed.), Proc. ICIAM 1991, SIAM, Philadelphia, 1992, 99–118.

[2] Cheng, Q., Liu, J.J., *Solving an inverse parabolic problem by optimization from final measurement data*, J. Computational and Applied Maths, Vol. 193 (2006), No. 1, 183–203.

[3] Fasano, A., Hömberg, D., Naumov, D., *On a mathematical model for laser-induced thermotherapy*, Appl. Math. Modelling, 34 (2010), 3831–3840.

[4] Fasano, A., Hömberg, D., Panizzi, L., *A mathematical model for case hardening of steel*, Math. Models Methods Appl. Sci., Vol. 19 (2009), 2101–2126.

[5] Hömberg, D., Krumbiegel, K., Rehberg, J., *Boundary coefficient control – a maximal parabolic regularity approach*, WIAS Preprint 1599, Berlin 2011.

[6] Hömberg, Volkwein, S., *Control of laser surface hardening by a reduced-order approach using proper orthogonal decomposition*, Math. Comput. Modelling, 38 (2003), 1003–1028.

[7] Hömberg, Yamamoto, M., *On an inverse problem related to laser material treatments*, Inverse Problems, Vol. 22 (2006), 1855–1867.

[8] Isakov, V., *Inverse Problems for Partial Differential Equations*, 2nd edition, Springer, 2006.

[9] Rösch, A., *Identification of nonlinear heat transfer laws by optimal control*, Numer. Funct. Anal. Optim. 15 (1994), no. 3-4, 417–434.

[10] Rösch, A., Tröltzsch, F., *An optimal control problem arising from the identification of nonlinear heat transfer law*, Arch. Control Sci, Vol. 1 (1992), no. 3-4, 183–195.

[11] Roggan, A., *Dosimetrie thermischer Laseranwendungen in der Medizin: Untersuchung der speziellen Gewebeeigenschaften und physikalisch-mathematische Modellbildung, Fortschritte in der Lasermedizin*, Vol. 16, Hüthig Jehle Rehm, Landsberg/Lech, 1997.

[12] Tröltzsch, F., *Optimal Control of Partial Differential Equations: Theory, Methods and Applications*, American Mathematical Society, 2010.

[13] Visintin, A., *Mathematical models of solid–solid phase transitions in steel*, IMA J. Appl. Math. **39** (1987), 143–157.